ACS APPLIED MATERIALS & INTERFACES

Letter

www.acsami.org

# Holographic Photopolymer Linear Variable Filter with Enhanced Blue Reflection

Tania Moein, Dengxin Ji, Xie Zeng, Ke Liu, Qiaoqiang Gan,* and Alexander N. Cartwright*

Department of Electrical Engineering, University at Buffalo, The State University of New York, Buffalo, New York 14260, United States

Supporting Information

**ABSTRACT:** A single beam one-step holographic interferometry method was developed to fabricate porous polymer structures with controllable pore size and location to produce compact graded photonic bandgap structures for linear variable optical filters. This technology is based on holographic polymer dispersed liquid crystal materials. By introducing a forced internal reflection, the optical reflection throughout the visible spectral region, from blue to red, is high and uniform. In addition, the control of the bandwidth of the reflection resonance, related to the light intensity and spatial porosity distributions, was investigated to optimize the optical performance. The development of portable and inexpensive personal health-care and environmental multispectral sensing/imaging devices will be possible using these filters.

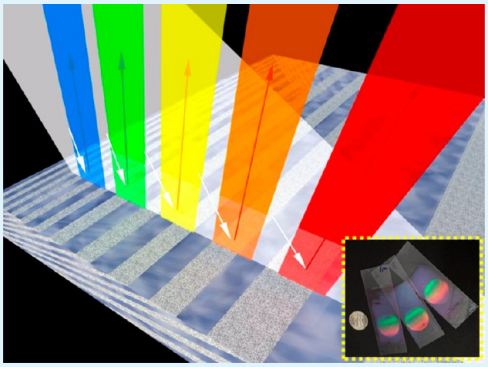

**KEYWORDS:** *holographic polymer dispersed liquid crystals, holographic photopatterning, graded rainbow-colored reflection grating*

## 1. INTRODUCTION

Multispectral and hyperspectral analyzers/imagers are widely used in remote sensing for applications ranging from environmental, agricultural and climate monitoring[1,2] to microscopy and bioimaging.[3−7] The ultimate costs of commercial devices for these applications are driven, at least partly, by the spectral resolution that is required. Moreover, the cost of tunable optical spectral filtering systems generally scales with the desired wavelength range and wavelength resolution. Generally, there are three kinds of spectral filtering systems used in multispectral imaging devices. The first system uses 5−8 separate high acuity color filters assembled in a large filter wheel to analyze the "true color" information in a scene. This is an expensive configuration to manufacture and results in large and bulky analyzer/imager systems. However, these systems are routinely used for multispectral imaging because of the achievable accuracy during spectral imaging. The second system consists of liquid crystal filters (LCF) that are employed to control the observation of the wavelength/color. This filter system is routinely used in bioimaging applications.[8,9] Unfortunately, the spectral response of these LCFs at different wavelength regions is not uniform. Specifically, the optical response in the blue wavelength region (400−500 nm) can have transmission less than 10%, limiting the application of LCF in many low-light imaging applications.[10] In addition, the dimensions of these LCFs cannot be easily miniaturized and also results in large and bulky imaging systems. The third spectral filtering system, comprised of linear variable filters (LVFs), was designed to provide small size and high transmission.[11] LVFs are compact graded color filters that are promising for the development of hand-held/portable color analyzers. The primary method used to produce LVFs is to deposit multiple layers of varied thickness, in a wedge fashion, using radically variable filter fabrication and ion-assisted deposition. The resulting multilayered structures, with different periods, create Fabry−Perot resonators with different resonant wavelengths. Although the LVFs can be scaled down in size and retain excellent transmission properties, they remain expensive.[11] Thus, none of these conventional spectral filter systems are suitable for the development of truly low-cost, hand-held devices. Consequently, the development of fabrication techniques to manufacture low-cost spectral filters with sufficient wavelength discrimination and high optical transmission could enable ubiquitous deployment of hyperspectral/multispectral imaging.

Recently, microfluidic channels were combined with colloidal photonic crystal structures to fabricate miniaturized spectrometers.[12] This method employs monodispersed colloidal particles that organize spontaneously into crystal lattices above a certain transition concentration depending on the interparticle interactions.[12−14] By controlling the particle diameter and contents of the suspension solutions, a photonic bandgap (PBG)[15] structure can be freely tuned in the visible spectral region. However, these colloidal PBG structures generally have intrinsic defects (e.g., vacancies and faults), leading to relatively low and nonuniform optical performance of the reflective

Received: December 2, 2013
Accepted: February 11, 2014
Published: February 11, 2014

  

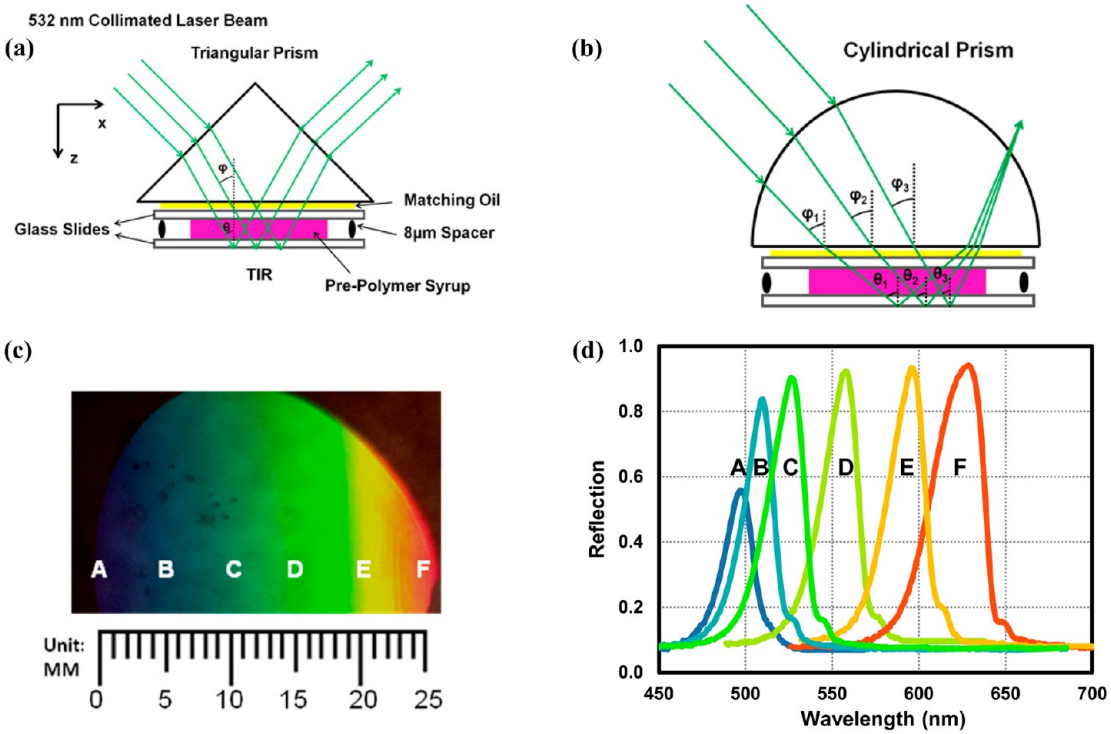


**Figure 1.** (a) Typical optical setup for conventional holographic photopatterning. The porous polymer PBG sample is prepared by sandwiching the prepolymer syrup between two parallel glass slides. (b) Modified optical setup based on a cylindrical lens to generate a graded holographic interference pattern along the *x*-axis from the incident and reflected beams. (c) Reflection image of a graded grating produced by the optical setup shown in b under white light illumination, and (d) its reflection spectrum at six different positions as indicated by letters of A, B, C, D, E, and F.

filters. More recently, we reported a one-step fabrication method for a graded reflection grating based on the holographic polymer dispersed liquid crystal (H-PDLC) material system.[16] The period of the grating at different positions along the structure could be changed gradually, resulting in a unique rainbow-colored reflection image in the same viewing angle. The cost of this filter system can be less than $10 for a 2 cm × 2 cm structure. Moreover, compared with the uniformity of the spectral performance of LCFs, the reflection response of our polymeric graded PBG gratings in the blue wavelength region is stronger (i.e., over 40−50%).[16] However, the reflection peak in the blue region (at ∼480 nm) was still lower than what was achieved at longer wavelengths where the averaged reflection efficiency was over 80%. Consequently, the objective of the work reported here is to understand the mechanism and further improve the reflectivity of the graded grating in the short wavelength region and to enable a rainbow colored reflection grating with reflection of over 80% throughout the visible wavelength range. This compact linear variable rainbow colored reflector can be integrated with portable multispectral imagers and therefore enable the development of personal health-care and environmental sensing devices.

## 2. CONVENTIONAL HOLOGRAPHIC PHOTOPATTERNED POLYMER PHOTONIC CRYSTAL STRUCTURES

This unique polymer linear variable filter consists of photonic crystal (PC) structures fabricated using a H-PDLC material system that is patterned using a holographic photopatterning technology. A summary of PCs, the material system and the fabrication method is provided below:

**PCs.** PC structures are periodic optical nano/micro-structures that are designed to provide a refractive index (RI) modulation that affects the motion of incident photons.[17] Essentially, they contain regularly repeating regions of high and low refractive indices. This RI modulation will change the transmission/reflection of light, i.e., certain wavelength bands cannot propagate through this structure. PCs are attractive structural materials for controlling and manipulating the flow of light and widely employed in thin film optics ranging from low or high reflection coatings on lenses, mirrors and optical filters to PC fibers for optical communications. Here, we exploit H-PDLC materials to develop low-cost variable period PCs.

**Materials.** H-PDLCs are a phase separation material system where the liquid crystals (LC) can form droplets, of controllable sizes, that are phase separated from the polymer-rich regions during the photopolymerization process.[18] Significant research in this material system has focused on the development of holographic optical elements that are low-cost, lightweight, and high performance. In the typical application, the LCs provide electric-field sensitive optical elements that enable the fabrication of switchable transmissive and reflective diffraction optics.[19] These structures are usually created by the coherent interference of laser radiation within a syrup containing a photoreactive monomer, a photoinitiator, co-initiator and the LC. Applications of these materials have included nano- and meso-particle organizers[20] and organic solvent vapor sensors.[21] It is believed that novel and promising biomedical applications are also achievable using these hybrid LC and polymer materials and devices.[22] More recently, intensely colored polymer films were created using colloidal assembly processes[23] based on the principles of structured color used by nature.[24] However, these films cannot be made

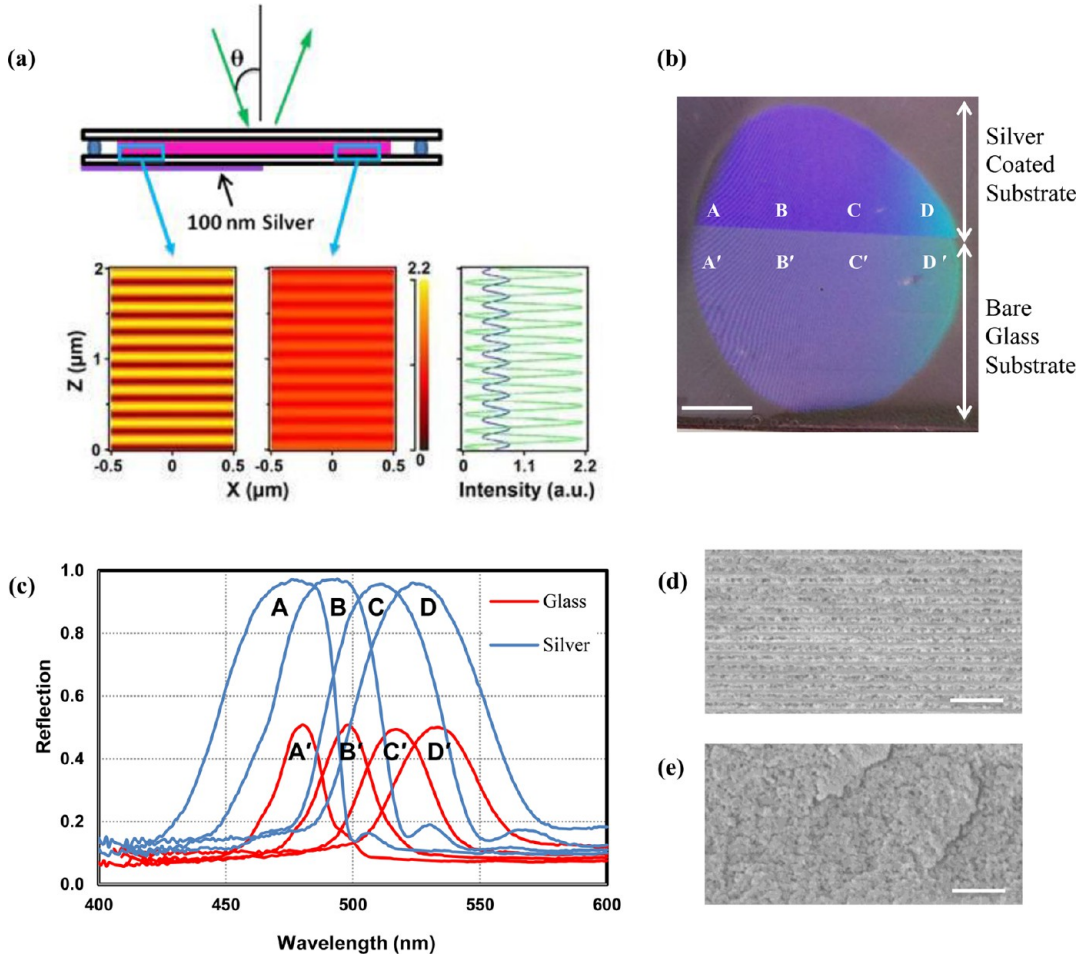


**Figure 2.** (a) Top panel: cross-sectional illustration of the polymer system with a half-glass/half-Ag bottom slide. Lower panel: numerical simulation of the reflected interference pattern from the Ag-coated and bare glass slide under the incident angle of 24°. (b) Photograph of a graded blue-green grating fabricated on a half-glass-half/Ag bottom slide under an incident angle of 5°. The scale bar indicates 5 mm. (c) Measured reflection along the four-pair positions indicated by A–D and A′–D′ in b. (d, e) Cross-sectional SEM images of polymer gratings at position A and A′, respectively. The scale bar is 1 $\mu$m.

multispectral in the same viewing angle,[23,25] as was demonstrated recently in our one-step holographic patterning technique to produce "rainbow" polymer gratings.[16]

**Photopatterning Technology.** Holographic lithography provides a simple and low-cost way to fabricate large areas of ordered structures.[26−28] A typical holographic lithography setup combines the techniques of holography and laser-induced polymerization in which photoresists or monomers are exposed to the spatial interference pattern introduced by coherent laser beams.[19,26−28] We have previously demonstrated that the constituents of the prepolymer syrup can have drastic effects on the resulting structures and, under appropriate conditions, result in periodic structuring of void-rich regions.[16,18] In our method, the photosensitive prepolymer syrup consists of a mixture of monomer, photoinitiator, co-initiator and solvents which is sandwiched between two glass slides with spacers that control the film thickness. Photopolymerization leads to higher polymerization in the high optical intensity regions of the interference pattern. More importantly, a postexposure ultraviolet curing procedure fully develops the structure and enhances the resulting phase separation between the polymer and the solvent. Upon opening the sandwiched sample, the solvent evaporates and leaves behind voids that result in a periodic refractive index modulation in the recording media. The spatial interference patterns, resulting in reflection gratings, can be readily achieved using a single beam configuration with a triangular prism which has been widely used in patterning of three-dimensional polymeric microstructures,[26−31] as illustrated in Figure 1a. In this geometry, the recording medium is placed in contact with the hypotenuse of the prism using index matching oil. The recorded optical pattern is formed by the interference between the incoming beam and its own total internally reflected beam at the bottom of the sample. The period of the interference pattern in the $z$-direction is determined by the incident angle (or its complementary angle), the refractive index of the recording material and the operational wavelength, as described by eq 1

$$\Lambda = \frac{m\lambda_{\mathrm{Bragg}}}{2n_{\mathrm{ave}}\sin\theta} \tag{1}$$

where. $\theta = \cos^{-1}[(n_{\mathrm{prism}}/n_{\mathrm{sample}})\cos(\varphi)]$ Here $\Lambda$ is the period of the PBG structure, $m$ is an integer representing the diffraction order of the Bragg reflector, $n_{\mathrm{ave}}$ is the average refractive index of the recording film, $\lambda_{\mathrm{Bragg}}$ is the PBG peak wavelength, $\varphi$ is the angle in the glass medium and $\theta$ is the scattering angle in the polymer syrup, as indicated in Figure 1a. The $z$-axis is chosen perpendicular to the glass slides and the $x$-axis parallel


dx.doi.org/10.1021/am405509t | ACS Appl. Mater. Interfaces 2014, 6, 3081−3087

to the glass slide. In recent years, we have successfully demonstrated highly reflective volume Bragg gratings[18] and nanoporous polymer photonic crystals[22] based on H-PDLC materials and this holographic photopatterning technology. When the triangular prism is replaced by a cylindrical lens, the propagation direction of the refracted light beam depends on the spatial location on the curved surface of the lens, as illustrated in Figure 1b. The complementary angle of the incident angle, $\theta$, within the film is slightly different at different positions on the recording media plane. Consequently, a continuous variation of $\theta$ is achieved by coupling the light through a curved lens surface, which results in a continuously varying period of the spatial interference pattern in the $x$-direction.[16] On the basis of this design principle, a graded porous polymer PC reflection grating can be fabricated. In this patterning, a collimated laser beam at 532 nm was used with the writing power density of 256 mW/cm$^2$. The incident angle was $\varphi_2 = 25°$. As shown in Figure 1c, an obvious rainbow-colored reflection was observed from the same viewing angle. However, as shown by the characterization results in Figure 1d, the reflection intensity in the blue region (i.e., ∼45% at 490 nm) is lower than at longer wavelengths (i.e., that over 80%). The main mechanism responsible for this nonuniform reflection performance can be interpreted as follows: As we explained in panels a and b in Figure 1, the periodic grating is formed by the interference pattern introduced by the total internal reflection (TIR) of the incident laser beam. The quality of the polymer-based PBG structure is determined by the modulation amplitude of the interference pattern which can be optimized when the intensities of the incident and reflected beams are identical. In our experiment, the incident angle varies due to the beam being focused through the cylindrical lens, as illustrated in Figure 1b. The incident angle, $\theta$, is estimated to be ∼24° in the blue edge (based on ray tracing modeling), which is much smaller than the critical angle at the glass/air interface (i.e., ∼41°). Consequently, the TIR condition cannot be met in the blue region of the graded grating structure, leading to a decreased reflection. The Fresnel reflection coefficient at the glass/air interface is calculated in Figure S1 in the Supporting Information. One can see that when the incident angle is larger than 41°, the reflection coefficients for all polarization states are 1. In contrast, when the incident angle is ∼24°, the reflection coefficients are 0.077 for s-polarized light ($R_s$), 0.018 for p-polarized light ($R_p$), and 0.047 for unpolarized light ($R$), respectively. In this case, the intensity ratio of the incident light to the reflected light is over 13:1 for s-polarized state in our experiment, resulting in the weak interference amplitude. To address this limitation, we can introduce a forced enhanced "TIR" to improve the reflection in the short wavelength region.

## 3. RESULTS AND DISCUSSION

**3.1. Reflection Enhanced Patterning Using Ag Mirror.** As illustrated by the upper panel in Figure 2a, we introduced a 100 nm thick silver (Ag) film on the bottom glass slide to enhance the reflection of the incident beam. Because of the excellent reflection property of the Ag mirror, a highly reflected beam is achieved for any incident angle. Therefore, the modulation of the interference pattern can be improved significantly, particularly at the positions where the TIR condition could not be met in the previous setup shown in Figure 1b. To demonstrate this enhanced interference pattern, we employ the rigorous coupled wave analysis method to model the interference pattern with/without the Ag reflector at the glass surface under the incident angle, $\theta$, of 24°. As shown in the lower panel of Figure 2a, the amplitude of the interference pattern is enhanced obviously with the Ag reflector, and the visibility of the interference pattern, $(I_{max} - I_{min})/(I_{max} + I_{min})$, is enhanced from 0.17 to 0.80. To validate this improved "TIR" method, we introduced a half-glass/half-Ag patterned glass slide as the bottom slide (see the central panel in Figure 2a) to fabricate a blue-green rainbow grating at the incident angle, $\varphi_2$, of 5°. One can see the reflection with the Ag-coated section is obviously improved. Quantitative measurement data are shown in Figure 2c. The net reflection peak in the blue region (around 480 nm) is improved significantly from ∼40% to over 90% (by subtracting the background reflection of ∼7%), confirming the improved interference patterning introduced by the Ag mirror. To further demonstrate the improved quality of the polymer grating, we characterize the cross-sectional scanning electron microscope (SEM) images of the polymer gratings on the Ag-coated part (see Figure 2d) and bare glass part (see Figure 2e), respectively, at position A and A′ as indicated in Figure 2b. The period of the pattern is ∼166.7 nm at this position. The highest frequency cut off of the grating period patterned by the laser at 532 nm can be obtained with the normal incident beam (i.e., $\varphi_2 = \theta = 0°$) with no cylindrical lens to focus the incident beam. As shown in Figure S2 in the Supporting Information, the peak of the reflection spectrum of a grating patterned with the normal incident light is at 472 nm. According to the microscopic characterization and analysis shown in Figure S2 in the Supporting Information, the highest frequency cut off is ∼158 nm. However, this is only the cut off under this incident wavelength (i.e., 532 nm). Shorter periods would require using another (shorter) wavelength laser or phase shift techniques. Therefore, we did not know the highest possible period that can be realized in this polymer material, which is still under investigation.

Clearly improved periodic grating structures were obtained on the Ag-coated part, validating the enhanced reflection pattering. However, another obvious phenomenon observed in Figure 2b is that the improved reflection bandwidth is broadened significantly. According to the measured data shown in Figure 2c, the bandwidths of the four positions measured in the enhanced "TIR" region were generally increased by approximately two times compared with the bare glass side (see details in Table 1). Although the reflection intensity is enhanced, this broadened bandwidth is not desired for certain optical filter applications, which will be analyzed and optimized below.

**Table 1. Bandwidth Measurement at Four Different Positions in the Glass and Silver-Coated Sides Along the $x$ Direction of the Grating Structure, As Indicated in Figure 2b**

| | positions | | | |
|---|---|---|---|---|
| | A (A′) | B (B′) | C (C′) | D (D′) |
| bandwidth (nm) silver-coated | 46 | 44 | 46 | 54 |
| bandwidth (nm) glass | 19 | 22 | 28 | 36 |

**3.2. Mechanism of the Broadened Reflection Peak and Optimization of the Amplitude.** To interpret the enhanced and broadened reflection peak in the blue-green linear variable grating shown in Figure 2b, we first analyze the phase separation process of the H-PDLC materials, as illustrated in Figure 3a. Because of the enhanced reflection intensity, the interference amplitude of the writing beam in the

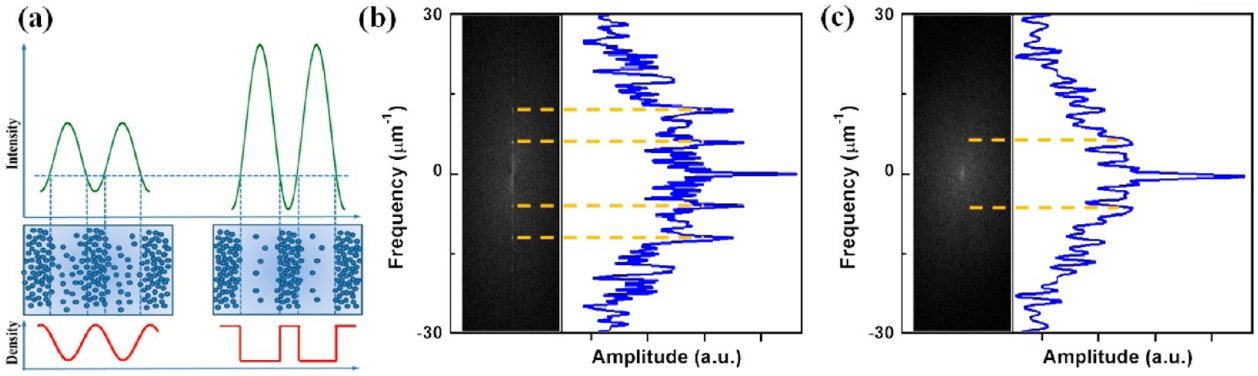


**Figure 3.** (a) Schematic illustration of the change of the phase-separated material distribution achieved by tuning the writing intensity and amplitude of the interference pattern. Fast Fourier transform (FFT) analysis of the images to determine the spatial frequency information of the cross-sectional SEM images of those gratings fabricated on the (b) Ag-coated substrates and (c) bare glass.

Ag-coated side is enhanced, resulting in a better phase separation of the polymer-rich region and void-rich region. Therefore, the distribution of the effective refractive index is closer to a "square-wave" shape with additional harmonic components (as illustrated in the lower panel of Figure 3a). To confirm this interpretation, we performed a fast Fourier transform (FFT) to analyze the spatial frequency information of the cross-sectional SEM images of those gratings fabricated on the half-Ag/half-glass substrate. As shown in Figure 3b, obvious harmonic frequency components at 6.0 $\mu m^{-1}$ (1st order), 12.0 $\mu m^{-1}$ (2nd order), and 17.7 $\mu m^{-1}$ (3rd order) were observed in the enhanced "TIR" region, confirming the "square-wave" distributed grating. While the grating on the glass side has only the first order component at 6.0 $\mu m^{-1}$, as shown in Figure 3c. According to classical Fourier optics,[32] the reflection of a square wave grating is broader than that of a sinusoidal wave grating. It is therefore clear that one has to suppress the high order harmonic components in the spatial refractive index distribution to optimize the reflection bandwidth of the linear variable polymer grating.

According to our previous studies,[33−35] it has been shown that the structural quality of the polymeric PBG patterns can be dictated by the writing amplitude, geometry, writing beam polarizations, etc. To obtain an improved linear variable polymer grating with narrower reflection peaks, we then controlled the writing beam intensity to reduce the higher harmonic components. In this photopatterning, we tuned the writing beam power density to fabricate the blue-green linear variable gratings and characterized their reflection spectra with $\varphi_2$ of 5°. Their full width at half-maximum (FWHM) and reflection peak amplitude at the wavelength of 490 nm are compared in Table 2. Considering the reflection amplitude and bandwidth of the reflection spectrum, the optimized blue-green rainbow grating is shown in Figure 4a fabricated by the power density of 10.24 mW/cm$^2$. The measured reflection spectra at the four positions along the grating are plotted in Figure 4b with the reflection peak in excess of 80% in the blue to green spectral region. Remarkably, the bandwidth is ∼23 nm, which is narrowed significantly compared with those shown in Figure 2c. To validate the suppressed high order harmonic components, the cross-sectional SEM image of the grating with reflection peak of 480 nm and its corresponding FFT image are shown in images c and d in Figure 4, respectively. One can see that only one clear harmonic component is obtained at the spatial frequency of 6.0 $\mu m^{-1}$, leading to the narrowed reflection peak.

**Table 2. Comparison of the FWHM and reflection Amplitude at the Wavelength of 490 nm of the Polymer Gratings Fabricated by Different Writing Beam Power Densities**

| | power density (mW/cm$^2$) | | | | | |
|---|---|---|---|---|---|---|
| | 256 | 60 | 23.2 | 10.2 | 3 | 1.0 |
| FWHM (nm) | 46 | 40 | 33 | 25 | 18 | 10 |
| Reflection (%) | 87 | 87 | 86 | 85 | 65 | 30 |

**3.3. Uniform Rainbow-Colored Grating.** Because of the enhanced TIR mechanism, a more reflective and narrower bandwidth polymeric linear variable filter can be realized by optimizing the writing beam intensity. Following this optimized photopatterning condition, we tuned the incident angle, $\varphi_2$, to 25° and fabricated a blue-red linear variable grating with the Ag-reflector and a writing power density of 10.24 mW/cm$^2$. As shown in Figure 5a, an improved blue-to-red rainbow-colored reflection was observed, with uniformly high reflection peaks over 80% from 470 to 630 nm (see Figure 5b). Moreover, the bandwidths at the six characterization spots (1-mm in diameter) are 20, 24, 28, 28, 26, and 27 nm, respectively, which are much narrower than the one patterned under an incident power density of 256 mW/cm$^2$ shown in Figure 2b. It should be noted that this complete characterization was performed 9 months after the original photopatterning. We also characterized the reflection spectra at four positions of the graded grating 11 months after the fabrication, as shown by dotted lines in Figure 5b. One can see that the optical response is almost unchanged (the slight difference may be attributed to the alignment error in our characterization), demonstrating the great stability of the chemical and photochemical properties of the graded filter under laboratory storage conditions (e.g., temperature: 25 °C, humidity: 10−30%). This stable, uniform and narrow spectral response of the one-step low-cost fabricated rainbow-colored linear variable filter is superior to the current commercially available bulky and nonuniform LCF[8,9] and expensive LVF devices.[11]

## 4. CONCLUSION

In conclusion, we successfully developed a low-cost method to produce uniform and high performance graded rainbow-colored holographic reflection gratings based on porous polymer materials. By introducing a highly reflective surface in the photopatterning process, the TIR limitation as a function

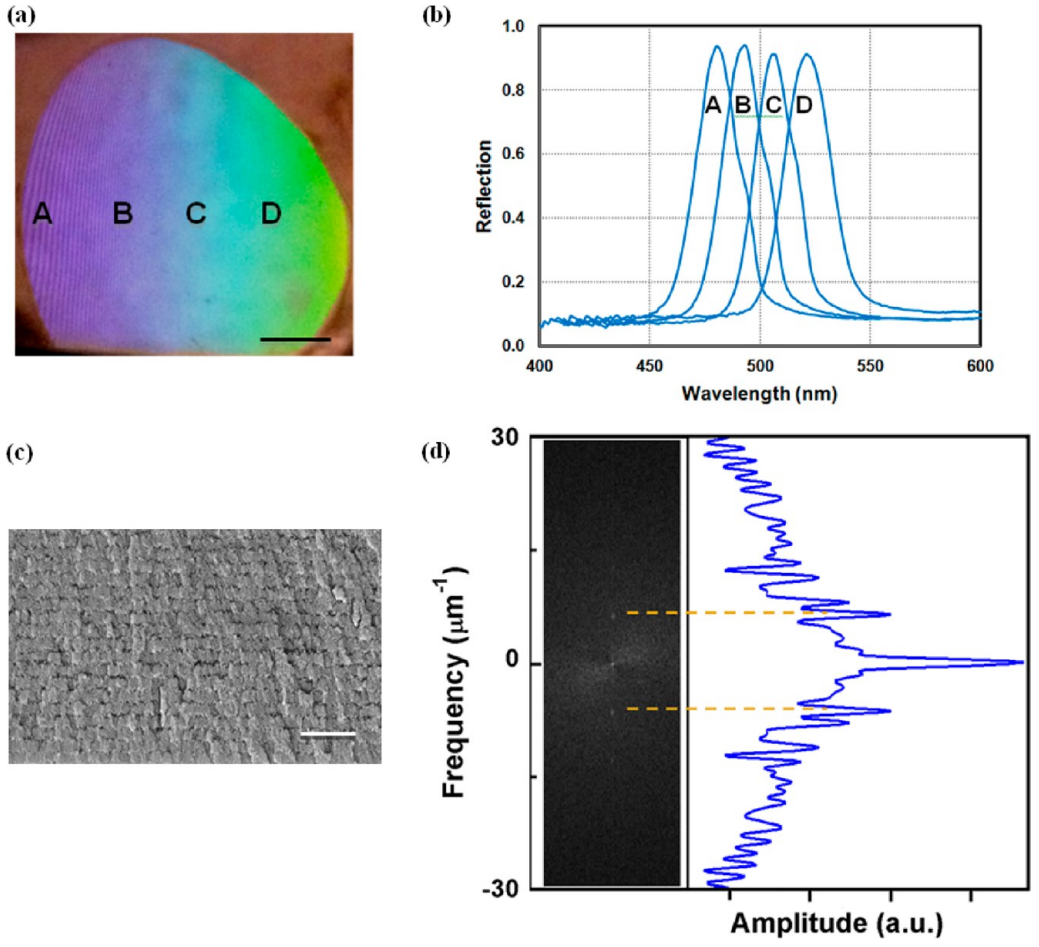


**Figure 4.** (a) Photograph of an optimized graded blue-green grating fabricated at a power density of 10.24 mW/cm$^2$. The scale bar indicates 5 mm. (b) Measured reflection spectra along the four positions indicated by A–D in a. (c) Cross-sectional SEM image of the polymer gratings along the position "A". The scale bar is 1 $\mu$m. (d) Fast Fourier transform (FFT) analysis to determine the spatial frequency information of the cross-sectional SEM image in c.

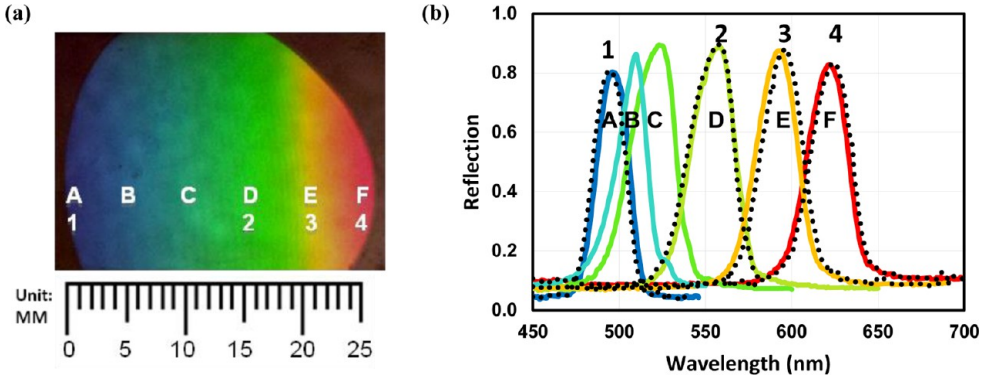


**Figure 5.** (a) Photograph of the optimized graded blue-red grating fabricated at an incident power density of 10.24 mW/cm$^2$. (b) Solid lines: measured reflection spectra at the six positions indicated by A–F in image a 9 months after the photopatterning. Dotted lines: measured reflection spectra at the four positions indicated by 1, 2, 3, 4 in image a 11 months after the photopatterning. Position accuracy is ±0.5 mm.

of the incident angle, $\theta$, was overcome and resulted in an improved fringe contrast that is independent of the angle $\theta$. Therefore, the reflection intensity at the blue region was improved significantly. By controlling the writing beam intensity, the spatial distribution profile of the polymerized region can be modified to reduce the spectral line width of the linear variable polymer grating due to the effective reduction in index modulation of the H-PDLC. The cross sectional morphology and its corresponding FFT image were both characterized to validate the design principle. This method provides a technique to fabricate graded optical elements, which can be integrated with portable cameras or cell phones easily and will enable the development of novel personal healthcare and environmental sensing devices[36] and anticounterfeiting signatures for banknotes[37] and security applications.[38]

## 5. EXPERIMENTAL SECTION

**Characterization.** To characterize the optical properties of the graded polymeric PGB structures, we used a monochromator (Acton-SpectraPro 2750) to select and scan the wavelength spectrum. The reflection spectrum from a silver mirror was measured as the reference. The sample was mounted on an adjustable stage (Newport 460A-XY Quick-Mount Linear Stage). By moving the stage, the reflection spectrum at different position along the polymer grating was measured.

## ■ ASSOCIATED CONTENT

### Supporting Information

Detailed calculation of Fresnel reflection coefficient of glass/air interface and the characterization of the high frequency of the patterned polymer grating. This material is available free of charge via the Internet at http://pubs.acs.org.

## ■ AUTHOR INFORMATION

### Corresponding Authors

*E-mail: qqgan@buffalo.edu.
*E-mail: anc@buffalo.edu

### Notes

The authors declare no competing financial interest.

## ■ ACKNOWLEDGMENTS

T.M., K.L., and A.N.C. acknowledge the support of the NIH NIBIB Grant Award 5R21EB009506 and the U.S. Air Force Office of Scientific Research Award FA95501010216. D.J., X.Z., and Q.G. were supported by the NSF Award ECCS1128086. T.M., K.L., A.N.C., D.J., X.Z., and Q.G. were supported by the SUNY Technology Accelerator Fund 62919.

## ■ REFERENCES

(1) Gee, C.; Bossu, J.; Jones, G.; Truchetet, F. *SPIE Newsroom* **2008**.
(2) Coffey, V. C. *Opt. Photonics News* **2012**, *23*, 18−24.
(3) Smith, Z. J.; Chu, K.; Espenson, A. R.; Rahimzadeh, M.; Gryshuk, A.; Molinaro, M.; Dwyre, D. M.; Lane, S.; Matthews, D.; Wachsmann-Hogiu, S. *PLOS One.* **2011**, *6*, e17150.
(4) Zoueu, J. T.; Ouattara, S.; Toure, A.; Safi, S.; Zan, S. T. *Proceedings of the 3rd ICTON Mediterranean Winter Conference*; Angers, France, Dec 10−12, 2009 ; IEEE: Piscataway, NJ, 2009; pp 1−7.
(5) Brydegaard, M.; Guan, Z.; Svanberg, S. *Am. J. Phys.* **2009**, *77*, 104−110.
(6) Zoueu, J. T.; Loum, G. L.; Haba, T. C.; Brydegaard, M.; Menan, H. *J. Appl. Sci.* **2008**, *8*, 2711−2717.
(7) Robinson, P.; Rajwa, B. P.; Bae, E.; Patsekin, V.; Roumani, A. M.; Bhunia, A. K.; Dietz, J. E.; Davisson, V. J.; Dundar, M. M.; Thomas, J.; Hirleman, E. D. *Opt. Photonics News* **2011**, *22*, 20−27.
(8) Woltman, S. J.; Jay, G. D.; Crawford, G. P., Eds. In *Liquid Crystals: Frontiers in Biomedical Applications*, 1st ed.; World Scientific Publishing: Singapore, 2007.
(9) Woltman, S. J.; Jay, G. D.; Crawford, G. P. *Nat. Mater.* **2007**, *6*, 929−938.
(10) *VariSpec Material Safety Data Sheet No. 010053A_01*; Perkin Elmer: Waltham, MA, 2013; http://www.spectralcameras.com/files/VariSpec_Brochure.pdf (accessed January 2014).
(11) *Linear Variable Filters*; Ocean Optics: Dunedin, FL, 2012; http://www.oceanoptics.com/Products/lvfslinearvariablefilters.asp (accessed January 2014).
(12) Kim, S.; Park, H.; Choi, J.; Shim, J.; Yang, S. *Adv. Mater.* **2010**, *22*, 946.
(13) Kim, S.; Jeong, W.; Hwang, H.; Yang, S. *Angew. Chem., Int. Ed.* **2011**, *50*, 11649.
(14) Luo, Z.; Zou, C.; Syed, S.; Syarbaini, L. A.; Chen, G. *Colloid Polym. Sci.* **2012**, *290*, 141.
(15) Kim, S.; Lee, S. Y.; Yang, S.; Yi, G. *NPG Asia Mater.* **2011**, *3*, 25.
(16) Liu, K.; Xu, H.; Hu, H.; Gan, Q.; Cartwright, A. N. *Adv. Mater.* **2012**, *24*, 1604−1609.
(17) Joannopoulos, J. D.; Johnson, S. G.; Winn, J. N.; Meade, R. D. In *Photonic Crystals: Molding the Flow of Light*, 2nd ed.; Princeton University Press: Princeton, NJ, 2008.
(18) Hsiao, V.; Yong, K.; Cartwright, A. N.; Wihart, M. T.; Prasad, P. N.; Lloyd, P. F.; Bunning, T. J. *J. Mater. Chem.* **2009**, *19*, 3998.
(19) Bunning, T. J.; Natarajan, L. V.; Tondiglia, V. P.; Sutherland, R. L. *Annu. Rev. Mater. Sci.* **2000**, *30*, 83−115.
(20) Vaia, R. A.; Dennis, C. L.; Natarajan, L. V.; Tondiglia, V. P.; Tomlin, D. W.; Bunning, T. J. *Adv. Mater.* **2001**, *13*, 1570.
(21) Hsiao, V.; Kirkey, W. D.; Chen, F.; Cartwright, A. N.; Prasad, P. N.; Bunning, T. J. *Adv. Mater.* **2005**, *17*, 2211.
(22) Woltman, S. J.; Jay, G. D.; Crawford, G. P. *Nat. Mater.* **2007**, *6*, 929−938.
(23) Finayson, C. E.; Spahn, P.; Snoswell, D.; Yates, G.; Kontogeorgos, A.; Haines, A. I.; Hellmann, G. P.; Baumberg, J. J. *Adv. Mater.* **2011**, *23*, 1540.
(24) Kinoshita, S. *Structural Colors in the Real of Nature*; World Scientific Publishing: Singapore, 2008.
(25) Braun, P. V. *Nature* **2011**, *472*, 423−424.
(26) Lu, C.; Lipson, R. H. *Laser Photonics Rev.* **2010**, *4*, 568−580.
(27) Xia, D.; Ku, Z.; Lee, S. C.; Brueck, S. R. J. *Adv. Mater.* **2011**, *23*, 147−179.
(28) BRUECK, S. R. J. *IEEE* **2005**, *93*, 1704−1721.
(29) Bunning, T. J.; Natarajan, L. V.; Tondiglia, V. P.; Sutherland, R. L. *Annu. Rev. Mater. Sci.* **2000**, *30*, 83−115.
(30) Natarajan, L. V.; Shepherd, C. K.; Brandelik, D. M.; Sutherland, R. L.; Chandra, S.; Tondiglia, V. P.; Tomlin, D.; Bunning, T. J. *Chem. Mater.* **2003**, *15*, 2477−2484.
(31) Moon, J. H.; Yang, S. *J. Macromol. Sci., Part C: Polym. Rev.* **2005**, *45*, 351−373.
(32) Goodman, J. W. In *Introduction to Fourier Optics*, 3rd ed.; Roberts & Co: Englewood, CO, 2005.
(33) Hsiao, V.; Lin, T.; He, G.; Cartwright, A. N.; Prasad, P. N.; Natarajan, L.; Tondiglia, V.; Bunning, T. J. *Appl. Phys. Lett.* **2005**, *86*, 131113.
(34) Hsiao, V.; White, T. J.; Cartwright, A. N.; Prasad, P. N.; Guymon, C. A. *Eur. Polym. J.* **2010**, *46*, 937.
(35) Hsiao, V. Optical Nanofabrication of Photopolymer Based Photonic Bandgap Structures: Materials and Applications. Ph.D. Thesis, The State University of New York at Buffalo, Buffalo, NY, August 2005.
(36) Yi, D.; Wang, C.; Qi, H.; Kong, L.; Wang, F.; Adibi, A. *IEEE Trans. Biomed. Eng.* **2011**, *58*, 736−740.
(37) Chalmers, J. M.; Edwards, H. G. M.; Hargreaves, M. D., Eds. In *Infrared and Raman Spectroscopy in Forensic Science*, 1st ed.; John Wiley and Sons: New York, 2012.
(38) Rowe, R. K.; Nixon, K. A.; Butler, P. W. *Multispectral Fingerprint Image Acquisition*; Ratha, N. K.; Govindaraju, V., Eds.; *Advances in Biometrics*; Springer: New York, 2008.